Proceedings of the ASME 2007 International Design Engineering Technical Conferences & Computers and Information in Engineering Conference
IDETC/CIE 2007
September 4-7, 2007, Las Vegas, Nevada, USA

DETC2007-35315

Nonlinear Model Based Estimation of Rigid-Body Motion via an Indirect Measurement of An Elastic Appendage

M. Mor *, A. Wolf, and O. Gottlieb

Technion – Israel Institute of Technology
Dept. of Mechanical Engineering
Haifa 32000, Israel.

ABSTRACT

In this paper we develop and implement a nonlinear model based procedure for estimation of rigid body motion via an indirect measurement of an elastic appendage. We demonstrate the procedure by motion analysis of a compound planar pendulum from indirect optoelectronic measurements of markers attached to an elastic appendage that is restrained to slide along the rigid-body length. We implement a Lagrangian approach to derive a theoretical nonlinear model that consistently incorporates the generalized forces acting on the system. Identification of the governing linear and nonlinear system parameters is obtained by analysis of frequency and damping backbone curves obtained from controlled experiments of the decoupled system elements. Comparison of an independently measured rotation angle to that obtained by the model-based estimation procedure enables evaluation of the procedure accuracy and its advantages over standard noninvasive methods.

Keywords: coupled nonlinear elastic-rigid body dynamical system, marker-based motion, and model based estimation.

1. INTRODUCTION

The World Health Organization estimates that several hundred million people already suffer from bone and joint diseases, with dramatic increases expected due to a doubling in the number of people over 50 years of age by 2020.
There are nearly 70 million Americans (one in four) suffering from arthritis and related conditions, and that number is expected to climb as baby boomers age.

Corresponding author: meravm@technion.ac.il

In accordance with this phenomenon, quantitative analysis of human movement has been recognized to be of great significance in both biomechanical and clinical studies.
Knowledge of the in-vivo movement of the joint is necessary for understanding its normal functionality as well as addressing and recognizing clinical abnormalities.
The most frequently used method for measurement of human locomotion involves placing markers on the skin of the analyzed segment[1]. Once markers are placed, an optoelectronic system composed of several high-frequency infra-red cameras can be employed to capture their location in space and time. However, estimation of the skeletal motion from the observed skin attached markers is significantly affected by the elasticity and nonlinear soft tissue deformation. This deformation results in erroneous calculation of the joint kinematics parameters [1-7] (e.g. joint center, axis of rotation).
Furthermore, because of its nature, the soft tissue response has a frequency content similar to that of the actual bone movement. Therefore, unlike instrument error, it is hard to deduce the bone motion by means of frequency based filtering technique [3, 8]. Consequently, skin motion is currently considered to be the primary source of error in evaluation of skeletal motion by noninvasive techniques [1-3, 9-11] .
To improve the accuracy of estimated bone motion, the development of methods for soft tissue artifact compensation is necessary. Several methods, both physical and numerical, have been proposed in the literature. Several of these methods are based on a least squares optimization of the marker cluster position and its orientation [1, 7, 11-13]. While these methods have shown initial promise, they remain to be independently verified relative to bone kinematics. Another type of method is based on a non-linear state-space estimation using an extended Kalman filter[4, 14]. However this method still lacks general validation and does not take into account any mechanical (e.g.

range of motion), or pathological (e.g. lost of degree of freedom) characteristics.

The purpose of this paper is to present a model based estimation procedure that yields the required rigid-body motion from the calibrated nonlinear response of an elastic element. The procedure is demonstrated by motion analysis of a compound planar pendulum from indirect optoelectronic measurements of markers attached to an elastic appendage that is restrained to slide along the pendulum. A Lagrangian approach was implemented to derive a theoretical nonlinear model that consistently incorporates the generalized forces acting on the system. Identification of the governing linear and nonlinear system parameters is obtained by analysis of the frequency and damping backbone curves obtained from experiments of the coupled and decoupled systems.

Comparison of a measured rotation angle to that obtained by the model-based estimation procedure enables evaluation of the procedure accuracy and its advantages over standard noninvasive methods.

2. EXPERIMANTAL ANALYSIS

Experimental Setup

The experimental system consists of a planar pendulum on which an elastic appendage is restrained to slide along (Fig. 1a, c). The pendulum is mounted on a fixed base via a shaft and a bearing. The shaft is free to rotate and is connected to the bearing via encoder via a coupler (Fig. 1b). Two markers (reflectors) are attached, one to the rigid pendulum and the other to the sliding mass.

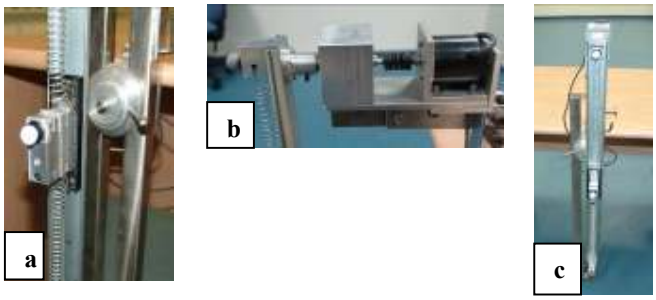

Fig 1: Experiment setup: (a) sliding mass (b) pendulum hinge (c) system setup.

During experiments, the pendulum was oscillating freely about the fixed base while the position of the two markers was measured using a Vicon Motion Capture System (Mx13) [14]. The Vicon Motion system is considered one of the gold standard system for biomechanics study and measurements. The reported capture system error [15] is 0.1pixels which is equivalent to 0.1-0.2mm (in 3D), based on dynamic calibration.

Free Vibration Decay

In this section we present results of both calibration test and an example of a coupled response. We first calibrate the rigid body with a fixed mass for identification of nonlinear drag.

Fig. 2a describes free vibration decay of a rigid body. Fig. 2b,c depicts the frequency and damping backbone curves, respectively.

The frequency backbone is obtained by plotting the instantaneous maximal (minimal) amplitudes ($A_{\max/\min}$) vs. their corresponding maximal (minimal) frequencies ($F_{\max/\min}$). We note that the maximal (minimal) frequency is obtained by the harmonic mean of the three opposite consecutive instantaneous periods: $F = (T_{i-1}^{-1} + T_i^{-1} + T_{i+1}^{-1})/3$ (1)

The damping backbone curve is obtained by the following equation deduced by a harmonic balance procedure [16,18]:

$$\varsigma = -(\dot{A}/A + F/2\dot{F})/4\pi \quad (2)$$

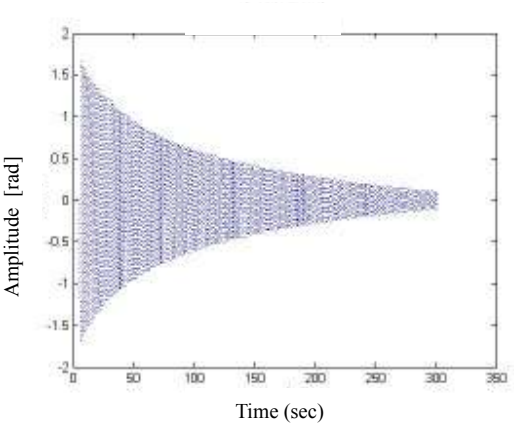

(a)

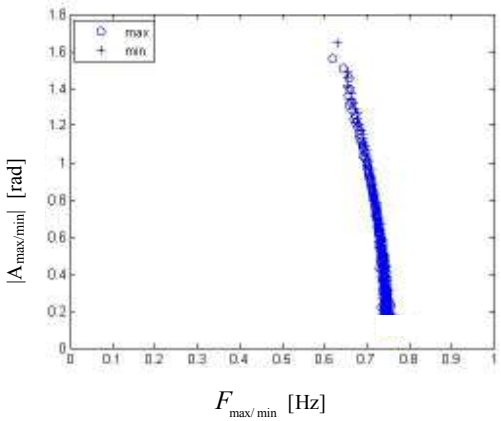

(b)

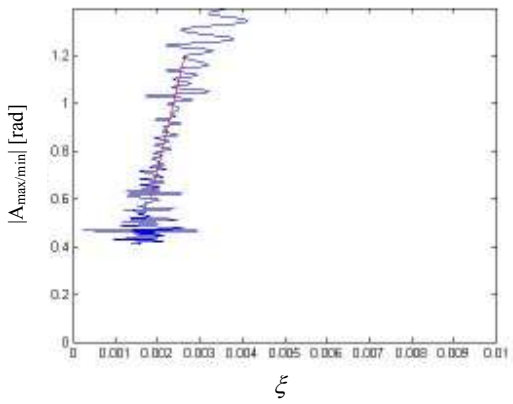

(c)

Fig 2: Pendulum decay:(a) angular free vibration, (b) frequency backbone (c) damping backbone.

Note that the frequency backbone is softening and yields a damped natural frequency of 0.763. The damping backbone curve reveals a linear component greater than $\varsigma_\theta = 0.001$.

The slider mass vibration on a horizontal rigid body is used to identify its stiffness and damping. Fig. 3a,b&c depicts free vibration decay, frequency and damping backbone curves, respectively.

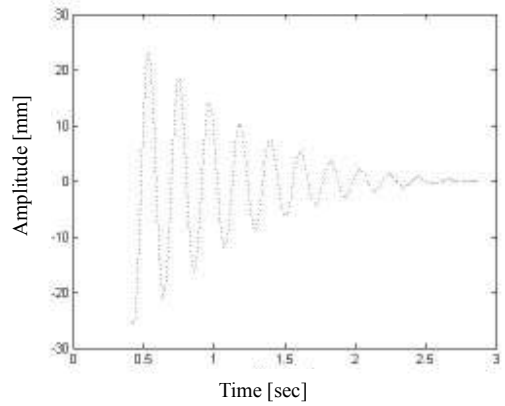

(a)

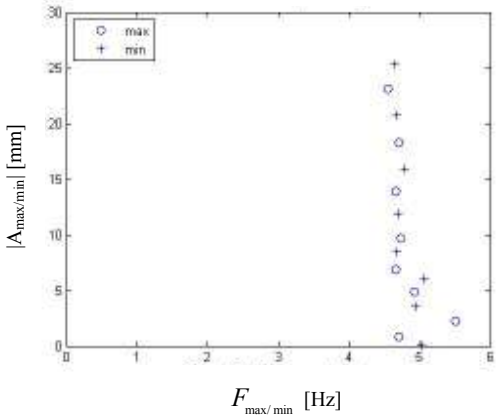

(b)

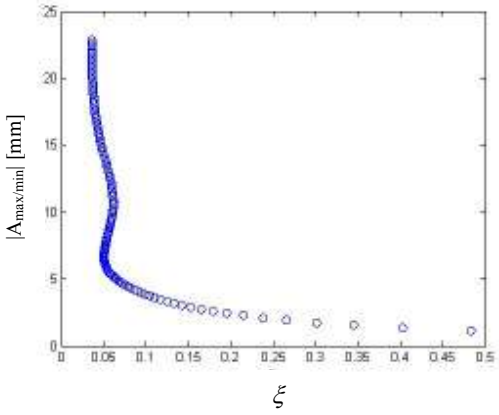

(c)

Fig 3: **Slider mass decay on a horizontal rigid body: (a) free vibration, (b) frequency backbone (c) damping backbone.**

Note that the frequency backbone curve yields a damped natural frequency of 4.63 Hz and that the damping backbone curve reveals both linear and dry friction components. The latter is evident by the almost linear decay rate in Fig.3a and by the hyperbolic relationship between amplitude and damping in Fig. 3c. The coupled rigid body and slider free vibration decay are depicted in Fig 4,5 respectively.

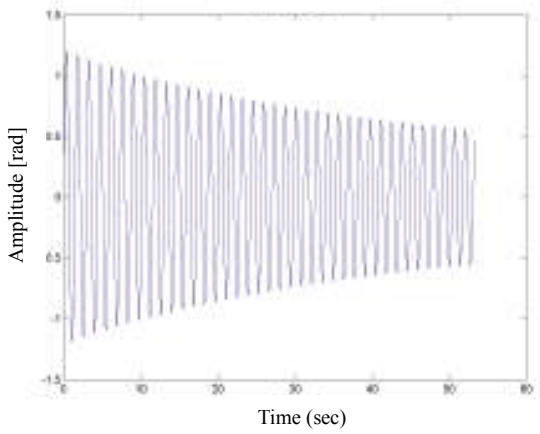

(a)

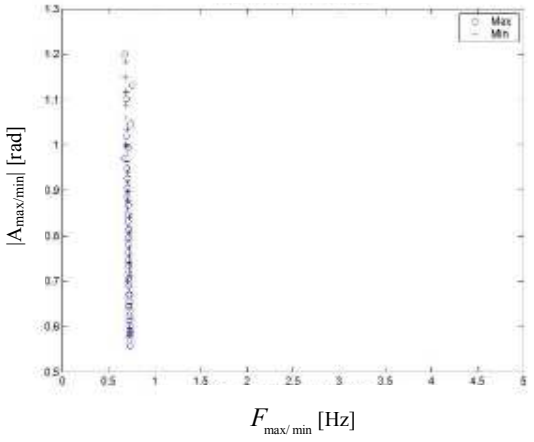

(b)

Fig 4: Coupled motion pendulum vibration: (a) angle [rad] , (b) frequency response backbone curve.

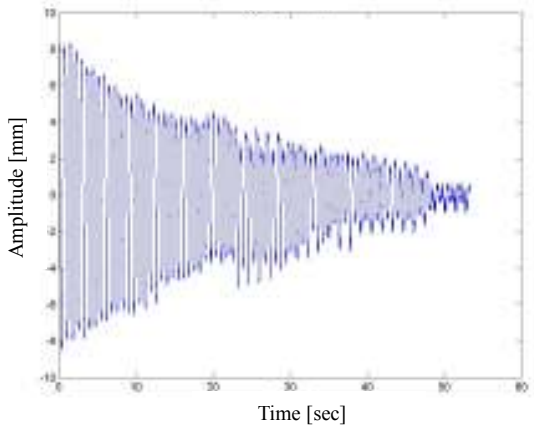

(a)

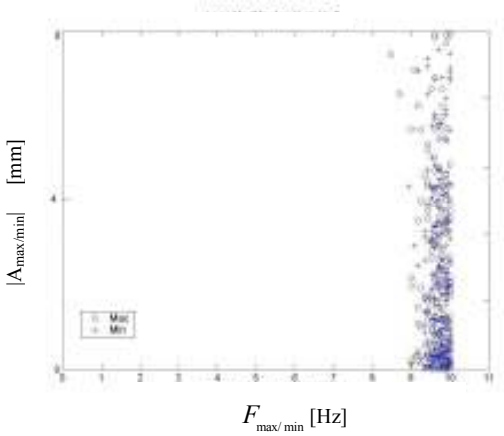

(b)

Fig 5: Coupled motion sliding mass vibration: (a) free vibration decay, (b) frequency response backbone curve.

Note that the rigid body decay appears similar to the calibration in Fig.2. However, the coupled slider decay in Fig.5 is more complex than that in Fig.3

3. THEORETICAL ANALYSIS

3.1. The Dynamical System

A Lagrangian approach [17] was implemented to deduce a theoretical model for the dynamical system of Fig.1. We define the elongation (r(t)) and angle ($\theta(t)$) as two generalized coordinates. The kinetic and potential energies of the dynamical system are:

$$\mathrm{KE} = \frac{1}{2}\left[\left(\mathrm{J_c} + \mathrm{MR_c^2} + \mathrm{I_c}\right)\dot{\theta}^2 + \mathrm{m}\left(\dot{\mathrm{r}}^2 + \mathrm{r}^2\dot{\theta}^2\right)\right],$$
$$\mathrm{PE} = -\mathrm{MgR_c}\cos\theta - \mathrm{mgr}\cos\theta + \frac{1}{2}\mathrm{k_1}\left(\mathrm{r} - \mathrm{l_1}\right)^2 + \frac{1}{2}\mathrm{k_2}\left(\mathrm{l_1} + \mathrm{b} - \mathrm{r}\right)^2 \quad (3)$$

Where $\mathrm{R_c}, \mathrm{M}$ and $\mathrm{J_c}$ are the rigid body mass center, mass, and moment of inertia respectively. The sliding mass and its moment of inertia are m and $\mathrm{I_c}$ respectively. Finally, k_j $\mathrm{l_j}$, and b represent the elastic stiffness, unstretched length of the springs, and slider length respectively.

The generalized forces acting on the system are dissipative and include both a restoring air drag moment and viscoelastic damping:

$$\mathrm{Q_\theta^d} = -\mathrm{c_\theta}\dot{\theta} - \mathrm{d}\,|\,\dot{\theta}\,|\,\dot{\theta},$$
$$\mathrm{Q_r^c} = -\mathrm{c_r}\dot{\mathrm{r}} - \mu\mathrm{mg}\sin\theta\,\mathrm{sgn}(\dot{\mathrm{r}}) \quad (4)$$

Where $\mathrm{c_r}$, $\mathrm{c_\theta}$, $\mathrm{d} = (\mathrm{C_d}\rho\mathrm{A_p}\mathrm{R_c^3}/2)$ and μ are the viscoelastic, drag and Coulomb friction coefficients respectively. There is an additional dry friction contribution to the rigid body. However,

it is identified as small with respect to the drag and viscoelastic restoring forces, hence is not considered in this model.

The equations of motion are deduced from the energies in Eq.(3) and generalized forces in Eq.(4) , resulting in[17]:

$$\begin{aligned}&\left[\left(J_c + MR_c^2 + I_c\right) + mr^2\right]\ddot{\theta} + 2mr\dot{r}\dot{\theta} + \left(MgR_c + mgr\right)\sin\theta = Q_\theta^d \\ &m\left(\ddot{r} - r\dot{\theta}^2\right) - mg\cos\theta + k\left(r - l_1\right) - k_2 b = Q_r^c\end{aligned} \tag{5}$$

Where k is a combined elastic stiffness, i.e. $k = k_1 + k_2$.

Note that as expected, the stable equilibrium position ($\dot{r} = \dot{\theta} = 0$) of the rigid body and slider are $\theta^* = 0$ and $r^* = \frac{k_2 b + mg}{k} + l_1 = L$, respectively. Furthermore, we note that for negligible rigid body mass (M), the undamped dynamical system in Eq.(5), is reduced to the standard equations for an elastic pendulum [17].

Next, we normalize the system in Eq.(5) by replacing r(t) with the nondimensional relative elongation given by $q = (r - L)/L$, and by a time scale $\tau = \omega_s t$ where the scaling frequency $\omega_s^2 = g(MR_c + mL)/I_t$, and $I_t = \left(J_c + MR_c^2 + I_c + mL^2\right)$ The resulting nondimensional equations of motion are:

$$\begin{aligned}&\left[1 + \alpha(2+q)q\right]\theta_{\tau\tau} + 2\alpha\left(1+q\right)q_\tau\theta_\tau + \left(1+\beta q\right)\sin\theta = -\left(\delta_1 + \delta_2\,|\,\theta_\tau\,|\right)\theta_\tau \\ &q_{\tau\tau} - (1+q)\theta_\tau^2 + (\beta/\alpha)\left(\gamma q + 1 - \cos\theta\right) = -\eta q_\tau - \mu(\beta/\alpha)\,\mathrm{sgn}(q_\tau)\sin\theta\end{aligned} \tag{6}$$

Where the nondimensional system parameters are:

$$\begin{aligned}&\alpha = \left[1 + \left(J_c + MR_c^2 + I_c\right)/mL^2\right]^{-1} < 1 \\ &\beta = \left[1 + \left(M/m\right)\left(R_c/L\right)\right]^{-1} < 1 \\ &\gamma = \left(kL/mg\right) = \left(1 + kl_0/mg\right) > 1 \\ &\delta_1 = \left(R_c C_\theta / I_t\omega_s\right) = 2\zeta_\theta < 1 \\ &\delta_2 = \left(d/mL^2\right) = \left[\left(\rho A_p R_c/m\right)\left(R_c/L\right)^3 C_d/2\right] < 1 \\ &\eta = \left(C_r/m\omega_s\right) = 2\zeta_q\left(\beta\gamma/\alpha\right)^{1/2} < 1 \\ &\mu < 1\end{aligned} \tag{7}$$

Note that the mass parameters (α, β) are less than unity, the gravity parameter (γ) is greater than unity and the damping parameters ($\delta_{1,2}, \eta, \mu$) are less than unity. Furthermore, we would like to point out that selection of the system rigid body and slider masses completely defines both mass parameters so that they consist of an independent design parameter. Thus, this scaling enables reduction of the original dynamical system parameter space in Eq.(5) from eleven parameters ($M, R_c, J_c, m, I_c, g, k, l_1, c_r, c_\theta, d$) to seven governing nondimensional parameters describing the relative system mass (α), gravity (γ), linear and nonlinear drag ($\delta_{1,2}$), linear viscoelastic damping (η) and Coulomb friction (μ).

Linearization of the dynamical system in Eq.(6) reveals that the nondimensional natural frequencies are $\omega_\theta = 1$ and $\omega_q = \sqrt{\beta\gamma/\alpha}$. These correspond to the following dimensional natural frequencies:

$$\begin{aligned}&\Omega_\theta = \omega_s = \left[g\left(MR_c + mL\right)/\left(J_c + MR_c^2 + I_c + mL^2\right)\right]^{1/2} \\ &\Omega_r = \omega_q\omega_s = \left[k/m\right]^{1/2}\end{aligned} \tag{8}$$

Note that for a negligible rigid body mass, the angular natural frequency reduces to that of a mathematical (lumped mass) elastic pendulum ($\Omega_\theta = \sqrt{g/L}$) which is always smaller than that of the elastic tether (Ω_r). Furthermore, both linear angular damping and linear viscoelastic damping are readily determined by their critical damping ratios $\zeta_\theta = \delta_1/2$ and $\zeta_q = \eta(\beta\gamma/\alpha)^{-1/2}/2$, respectively.

The free vibration decay of the coupled system is clearly governed by the relationship between its natural frequencies $\left(\omega_q/\omega_\theta\right)$. Conditions for internal resonance ($\omega_q \sim p\cdot\omega_\theta$, where p is in integer) will define the nature of the decay which will be smooth or of a quasiperiodic nature (e.g. $\omega_q \sim 2\omega_\theta$).

3.2. A Nonresonant Equivalent Pendulum Equation

An equivalent pendulum equation is readily deduced for nonresonant ($\omega_q \neq p\cdot\omega_\theta$) conditions where the elastic frequency is much larger than that of the pendulum ($\omega_q > p\cdot\omega_\theta$). We also assume that the slider damping is negligible for finite angular displacement. Thus, as the elastic force is much larger than its corresponding inertia, an equivalent kinematic relationship is obtained for the elongation as a function of angular velocity and displacement:

$$\tilde{q} = \left[\theta_\tau^2 - \frac{\beta}{\alpha}\left(1 - \cos\theta\right)\right]\left(\frac{\beta}{\alpha}\gamma - \theta_\tau^2\right)^{-1} \tag{9}$$

Substitution of this modified elongation ($\tilde{q} = \tilde{q}(\theta)$) into the pendulum equation Eq.(6a) yields an equivalent single degree of freedom pendulum equation of motion:

$$\left[1+\alpha(2+\tilde{q})\tilde{q}\right]\theta_{\tau\tau}+\left(1+\beta\tilde{q}\right)\sin\theta=-\left(\delta_1+\delta_2\,|\,\theta_\tau\,|\right)\theta_\tau \qquad (10)$$

4. MODEL BASED ESTIMATION OF RIGID BODY MOTION

4.1 Identification of Experimental System Parameters

The equation of motion for the planar pendulum is deduced from Eq.(5):

$$\ddot{\theta}+\omega_n^2\sin\theta=-\hat{\delta}_1\dot{\theta}-\hat{\delta}_2\dot{\theta}\left|\dot{\theta}\right| \qquad (11)$$

where

$\omega_n^2=(m+M)gR_C/I_t$, $\hat{\delta}_2=d/I_t$, $\hat{\delta}_1=2\varsigma_\theta\omega_n$.

The linear drag parameter ς_θ is identified using a logarithmic fitting of the maximum angular free vibration amplitude: $\varsigma_\theta=0.002$.

The system total moment of inertia was identified based on the dynamical system in Eq.(9) and frequency response backbone curve as $I_t=0.1554\ \ [kg\cdot m]$.

The pendulum nonlinear damping parameter was identified using an equivalent formula [16]:

$$A^2=4\left[1-\sqrt{1-3\left(3\pi/4\right)^2\left(1/6\omega_\theta^2\hat{\delta}_2^2\right)\left(\xi_\theta\omega_\theta-\hat{\delta}_1/2\right)^2}\right] \qquad (12)$$

A,ξ_θ were obtained from the damping response backbone curve (Fig 2).

The linear damping parameter of the coupled system Eq.(6): $\delta_1=2\xi_\theta=0.004$.

In order to get a good numerical fit, the nonlinear damping parameter was modified: $\hat{\delta}_2=0.001$.

Due to different normalization, the nonlinear damping parameter of the coupled system is $\delta_2=\hat{\delta}_2 I_t/mL^2=0.0014$.

The equation of motion for the slider mass vibration on a horizontal rigid body is deduced from Eq.(5):

$$\ddot{x}+\omega_n^2 x=-2\xi_1\omega_n\dot{x}-\mu g\,\mathrm{sgn}(\dot{x}) \qquad (13)$$

The Coulomb friction was identified based on dynamical system in Eq.(13) and the damping response backbone curve (Fig 3) as $\mu=A\pi\omega_n^2\xi_1(2g)^{-1}=0.0477$.

The linear damping parameter ς_q was identified by a logarithmic fit of the maximum free vibration amplitude for the unrestrained mass: $\varsigma_q=0.0008$.

The gravity parameter γ was identified based on the free vibration of the coupled system and the mass parameters: $\left(\omega_q/\omega_\theta\right)^2=\beta\gamma/\alpha$,

where $\alpha=0.073$; $\beta=0.0985$; $\omega_q/\omega_\theta=12.8$.

Therefore, the estimated gravity parameter is $\gamma=121.76$.

4.2 Estimation of Rigid Body Motion

i) Coupled system

Two sets of slider damping parameters were evaluated.

The guidelines for choosing these parameters were the fit of the pendulum cycles and the nondimensional slider vibration: $q(\tau=100)=0.01$.

The first model is based on linear damping and Coulomb friction parameters identified in section 4.1. (Fig. 6)

In the second model the Coulomb friction was neglected and a larger linear damping parameter ς_q was chosen ($\varsigma_q=0.001$) (Fig 7).

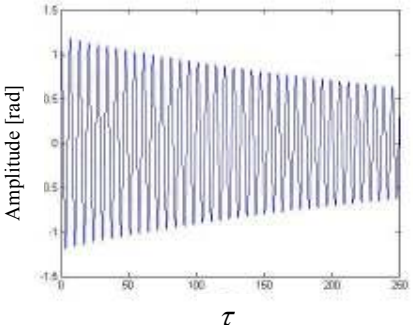

(a)

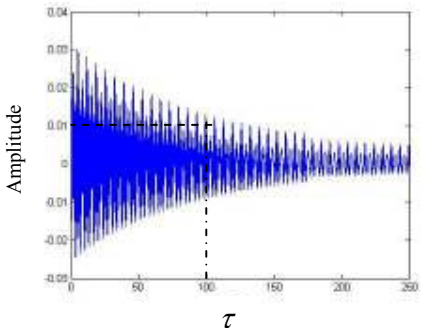

(b)

Fig 6: **Coupled system model (1)** $\mu=0.0477,\varsigma_q=0.0008$ **:**
(a) pendulum angle [rad], (b): slider mass decay.

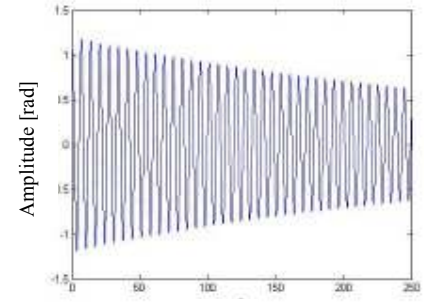

(a)

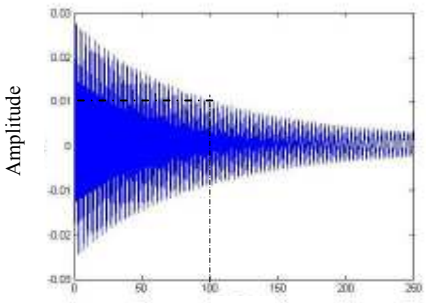

(b)

Fig 7: Coupled system model (2) $\mu = 0, \varsigma_q = 0.001$ **:**
(b) pendulum angle [rad], (b): slider mass decay.

ii) Nonresonant equivalent pendulum equation

The proposed nonresonant model can estimate the pendulum angle (Fig. 8) but cannot reproduce the slider vibration as Eq.(9) does not include any damping components.

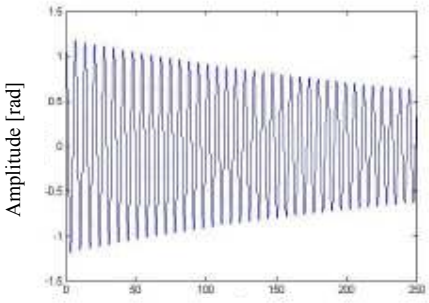

Fig 8: Nonresonant equivalent model: pendulum angle [rad].

4.3 Accuracy of the Estimated Response

In order to evaluate the accuracy of the proposed method, a relative error is defined as:

$$E_{\%} = 100 \cdot \left| |\theta_m| - |\theta_e| \right| / |\theta_m| \qquad (12)$$

Where θ_m , θ_e are the measured and estimated minimal angular amplitudes, respectively.

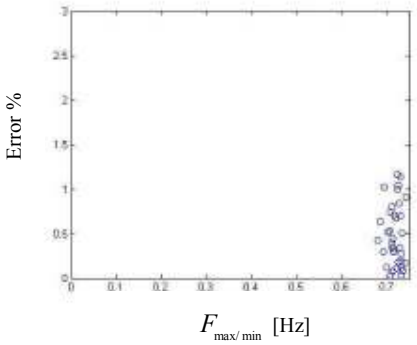

(a)

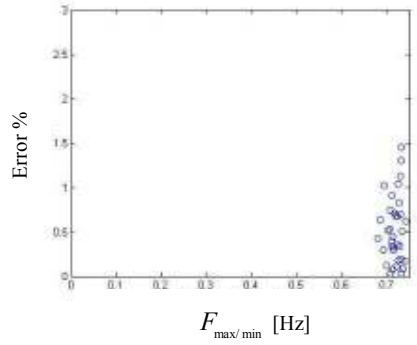

(b)

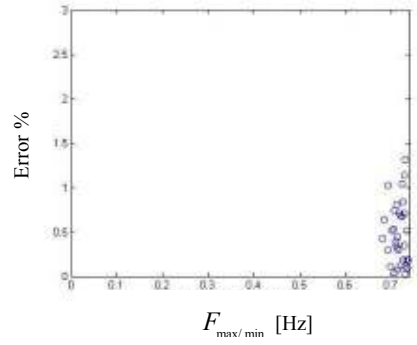

(c)

Fig 9: Error analysis: (a) coupled system model (1), (b) coupled system model (2), (c) nonresonant equivalent model

Note that the magnitude of error levels in Fig.9 reveals that the proposed method is effective in estimating the rigid body position from an indirect measurement of the elastic appendage. A maximum error of 1.5% was obtained in both the coupled model without Coulomb friction and in the nonresonant model. The model with both linear damping and Coulomb friction reveals of a maximum error of 1.2% (Fig. 9a).

5. CLOSING REMARKS

In this paper we have derived a nonlinear procedure for model based estimation of rigid-body motion via an indirect measurement of an elastic appendage. This model is a first step towards development of a method that will enable estimation of biomechanical measurements of bone and joint motion, based on surface markers placed on the skin.

The procedure was demonstrated by motion analysis of a compound planar pendulum from indirect optoelectronic measurements of markers attached to an elastic appendage that is restrained to slide along the rigid –body length. Results indicate a 1.2% error between measured motion and estimated motion of the pendulum resulting from the indirect optoelectronic measurements of the elastic appendage.

Future research will incorporate nonlinear hyperelastic polymer springs which better represent skin deformation

6. REFERENCES

1. T.P. Andriacchi , E.J.Alexander, M.K. Toney , C. Dyrby and J. Sum: '*A Point Cluster Method for In Vivo Motion Analysis: Applied to a Study of Knee Kinematics'*. Journal of Biomechanics Engineering, 1998. **120**: p. 743-749.
2. K. Manal, I.McClay Davis, B.Galinat and S.Stanhope: '*The accuracy of estimating proximal tibial translation during natural cadence walking: one vs.skin mounted targets'*. Clinical Biomechanics, 2003. **18**: p. 123-131.
3. A. Cappello, R.Stagni , S. Fantozzi and A. Leardini: *'Soft Tissue Artifact Compensation in Knee Kinematics by Double Anatomical Landmark Calibration: Performance of a Noval Method During Selected Motor Tasks'*. IEEE Transactions on Biomedical Engineering, 2005. **52**(6): p. 992-998.
4. P. Cerveri, M.Rabuffetti, A. Pedotti, and G.. Ferrigno: '*Real-time human motion estimation using biomecahnical models and non-linear state-space filters'*. Mediacl & Biological Engineering & Computing, 2003. **41**: p. 109-123.
5. C. Reinschmidt, A.J.van den Bogert , B.M. Nigg, A. Lundbergt and N. Murphy: '*Effect of Skin Movement on the Analysis of Skeletal Knee Joint Motion During Running'*. Journal of Biomechanics, 1997. **30**(7): p. 729-732.
6. J.H. Ryu, N.Miyata .,M. Kouchi, M. Mochimaru and K.H. Lee: '*Analysis of Skin Movements with Respect to Bone Morions using MR Images'*. International Journal of CAD/CAM, 2003. **3**(2): p. 61-66.
7. L. Che'ze, B.J. Fregly, and J. Dimnet: '*A solidification procedure to facilitate kinematic analysis based on video system data'*. Journal of Biomechanics, 1995. **28**: p. 879-884.
8. A. Leardini, L.Chiari., U.D. Croce and A. Cappozzo: '*Human movement analysis using stereophotogrammetry Part 3. Soft tissue artifact assessment and compensation'*. Gait & Posture, 2005. **21**: p. 212-225.
9. A. Cappozzo, F. Catani, A. Leardini,, M.G. Benedetti, and U.D. Croce: '*Position and orientation in space of bobes during movement: experimental artefacts'*. Clinical Biomechanics, 1996. **11**: p. 90-100.
10. J.P. Holden, J.A. Orsini, K.L Siegel, T.M. Kepple, L.H. Gerber and S.J. Stanhope: '*Surface movement error in shank kunematics and kinetics during gait'*. Gait & Posture, 1997. **5**: p. 217-227.
11. J. Eugene and T.P.A. Alexander: '*Correcting for deformation in skin-based marker systems'*. Journal of Biomechanics, 2001. **34**: p. 355-361.
12. A. Cappozzo, A. Cappello, U.D Croce, and F. Prnsalfini: '*Surface marker cluster design criteria for 3-D bone movement reconstruction'*. IEEE Transactions on Biomedical Engineering 1997. **44**(12): p. 1165-1174.
13. T.-W. Lu , and J.J. O'connor: '*Bone position estimation from skin marker co-ordinates using global optimisation with joint constraints'*. Journal of Biomechanics, 1999. **32**: p. 129-134.
14. P. Cerveri, A.Pedotti and G.. Ferrigno: '*Non-invasive approach towards the in vivo estimation of 3D inter-vertebral movements: methods and preliminary results'*. Medical Engineering & Physics, 2004. **26**: p. 841-853.
15. *Vicon Motion Systems and Peak Performance Inc.* 2007, http://www.vicon.com.
16. L. Meirovitch, *Methods of Analytical Dynamics*. 1988: McGraw-Hill.
17. A.H. Nayfeh, and D.T. Mook, *Nonlinear Oscillations*. 1979: Wiley.
18. O.Gottlieb and M. Feldman: '*Application of Hilbert Transform-Based Algorithm for Parmeter Estimation of a Nonlinear Ocean System Roll Model'*. Journal of Offshore Mechanics and Arctic Engineering, 1997. **119**: p. 239-243.